JOURNAL OF BACTERIOLOGY, Jan. 2006, p. 587–598 Vol. 188, No. 2
0021-9193/06/$08.00+0 doi:10.1128/JB.188.2.587–598.2006

YdgG (TqsA) Controls Biofilm Formation in *Escherichia coli* K-12 through Autoinducer 2 Transport

Moshe Herzberg,[1] Ian K. Kaye,[1] Wolfgang Peti,[2] and Thomas K. Wood[1]*

Departments of Chemical Engineering and Molecular & Cell Biology, University of Connecticut, 191 Auditorium Road, Storrs, Connecticut 06269-3222,[1] and Department of Molecular Pharmacology, Physiology, and Biotechnology, Brown University, 70 Ship Street GE3, Providence, Rhode Island 02912[2]

Received 1 September 2005/Accepted 27 October 2005

YdgG is an uncharacterized protein that is induced in *Escherichia coli* biofilms. Here it is shown that deletion of *ydgG* decreased extracellular and increased intracellular concentrations of autoinducer 2 (AI-2); hence, YdgG enhances transport of AI-2. Consistent with this hypothesis, deletion of *ydgG* resulted in a 7,000-fold increase in biofilm thickness and 574-fold increase in biomass in flow cells. Also consistent with the hypothesis, deletion of *ydgG* increased cell motility by increasing transcription of flagellar genes (genes induced by AI-2). By expressing *ydgG* in *trans*, the wild-type phenotypes for extracellular AI-2 activity, motility, and biofilm formation were restored. YdgG is also predicted to be a membrane-spanning protein that is conserved in many bacteria, and it influences resistance to several antimicrobials, including crystal violet and streptomycin (this phenotype could also be complemented). Deletion of *ydgG* also caused 31% of the bacterial chromosome to be differentially expressed in biofilms, as expected, since AI-2 controls hundreds of genes. YdgG was found to negatively modulate expression of flagellum- and motility-related genes, as well as other known products essential for biofilm formation, including operons for type 1 fimbriae, autotransporter protein Ag43, curli production, colanic acid production, and production of polysaccharide adhesin. Eighty genes not previously related to biofilm formation were also identified, including those that encode transport proteins (*yihN* and *yihP*), polysialic acid production (*gutM* and *gutQ*), CP4-57 prophage functions (*yfjR* and *alpA*), methionine biosynthesis (*metR*), biotin and thiamine biosynthesis (*bioF* and *thiDFH*), anaerobic metabolism (*focB*, *hyfACDR*, *ttdA*, and *fumB*), and proteins with unknown function (*ybfG*, *yceO*, *yjhQ*, and *yjbE*); 10 of these genes were verified through mutation to decrease biofilm formation by 40% or more (*yfjR*, *bioF*, *yccW*, *yjbE*, *yceO*, *ttdA*, *fumB*, *yjiP*, *gutQ*, and *yihR*). Hence, it appears YdgG controls the transport of the quorum-sensing signal AI-2, and so we suggest the gene name *tqsA*.

Escherichia coli biofilms have hundreds of genes differentially expressed (5, 48, 56); hence, it is important to understand how the biofilm lifestyle is regulated so that bacteria may be controlled (4). In the absence of conjugation plasmids (47), it appears type I fimbriae are required for cells to attach and that motility is essential for biofilm formation, probably for initial interaction (overcoming repulsive forces) and swimming along the surface (43). Following attachment, extracellular polymers and adhesive factors are produced, including curli and the outer membrane protein Ag43 (*flu*) (11, 44). The microcolonies mature into complex architecture by synthesis of an extracellular polysaccharide matrix such as colanic acid in *E. coli* biofilms (12).

Cell signaling (quorum sensing) also is involved in biofilm formation as it controls the production and secretion of exopolysaccharides for *Vibrio cholerae* biofilms (21). *Vibrio harveyi* uses three quorum-sensing signals, including *N*-(3-hydroxybutanoyl)homoserine lactone, furanosyl borate diester (autoinducer 2 [AI-2]), and a signal, synthesized by CqsA, whose structure is unknown (23). *N*-(3-Oxododecanoyl)-L-homoserine lactone controls biofilm formation in *Pseudomonas aeruginosa* (14). A homoserine lactone signal was also found to control cell aggregation and biofilm formation of *Serratia liquefaciens* (32). AI-2 was found to regulate mixed-species biofilm formation by *Streptococcus gordonii* and *Porphyromonas gingivalis* (39) and also to increase the amount of microcolonies in early stages of biofilm formation by *Klebsiella pneumoniae* and to increase the total mature biofilm formed by 30 to 50% (2). We have found that the quorum-sensing disrupter (*5Z*)-4-bromo-5-(bromomethylene)-3-butyl-2(*5H*)-furanone of the alga *Delisea pulchra* inhibits *E. coli* biofilms by repressing the same suite of genes that are induced by AI-2 (49), which argues that AI-2 should directly stimulate *E. coli* biofilm formation. This has recently been shown by using enzymatically synthesized AI-2, which increases biofilm formation 30-fold in 96-well biofilm assays and in flow cells (19).

AI-2 induces transcription of the *lsrACDBFGE* operon of *Salmonella enterica* serovar Typhimurium, in which the first four genes encode an ATP-binding cassette-type import protein with high homology to the ribose transporter (62, 63). AI-2 is phosphorylated inside the cell by LsrK, and phosphorylated AI-2 induces inactivation of the *lsr* operon repressor LsrR (62, 69). Addition of sugars that are part of the phosphotransferase system increases AI-2 extracellular activity to its maximum level in the mid- to late-exponential phase (60) through a decrease in the cyclic AMP (cAMP) concentration (65). Once glucose is depleted, cAMP concentrations increase, the *lsr* operon is activated by cAMP, and AI-2 is internalized by cells

* Corresponding author. Mailing address: Departments of Chemical Engineering and Biology, Texas A & M University, 220 Jack E. Brown Building, College Station, TX 77843-3122. Phone: (979) 862-1588. Fax: (979) 845-6884. E-mail: Thomas.Wood@chemail.tamu.edu.

TABLE 1. *E. coli* strains and plasmids used in this study

Strain or plasmid	Genotype[a]	Reference
Strains		
V. harveyi BB170	Wild type	60
E. coli K-12 BW25113	*lacI*^{q} *rrnB*$_{T14}$ Δ*lacZ*$_{WJ16}$ *hsdR514* Δ*araBAD*$_{AH33}$ Δ*rhaBAD*$_{LD78}$	13
E. coli K-12 BW25113 Δ*ydgG*	K-12 BW25113 Δ*ydgG* Ω Km^r	1
E. coli K-12 BW25113 Δ*yfjR*	K-12 BW25113 Δ*yfjR* Ω Km^r	1
E. coli K-12 BW25113 Δ*bioF*	K-12 BW25113 Δ*bioF* Ω Km^r	1
E. coli K-12 BW25113 Δ*yccW*	K-12 BW25113 Δ*yccW* Ω Km^r	1
E. coli K-12 BW25113 Δ*yceO*	K-12 BW25113 Δ*yceO* Ω Km^r	1
E. coli K-12 BW25113 Δ*ttdA*	K-12 BW25113 Δ*ttdA* Ω Km^r	1
E. coli K-12 BW25113 Δ*yjbE*	K-12 BW25113 Δ*yjbE* Ω Km^r	1
E. coli K-12 BW25113 Δ*fumB*	K-12 BW25113 Δ*fumB* Ω Km^r	1
E. coli K-12 BW25113 Δ*gutQ*	K-12 BW25113 Δ*gutQ* Ω Km^r	1
E. coli K-12 BW25113 Δ*yjiP*	K-12 BW25113 Δ*yjiP* Ω Km^r	1
E. coli K-12 BW25113 Δ*yihR*	K-12 BW25113 Δ*yihR* Ω Km^r	1
E. coli K-12 BW25113 Δ*gutM*	K-12 BW25113 Δ*gutM* Ω Km^r	1
E. coli K-12 BW25113 Δ*ybcJ*	K-12 BW25113 Δ*ybcJ* Ω Km^r	1
E. coli K-12 BW25113 Δ*ybfG*	K-12 BW25113 Δ*ybfG* Ω Km^r	1
E. coli K-12 BW25113 Δ*citG*	K-12 BW25113 Δ*citG* Ω Km^r	1
E. coli K-12 BW25113 Δ*acrE*	K-12 BW25113 Δ*acrE* Ω Km^r	1
Plasmids		
pCM18	Em^r; pTRKL2-P$_{CP25}$RBSII-*gfp*3*-T$_0$-T$_1$	22
pCA24N	Cm^r; *lacI*^{q}	1
pCA24N *ydgG*$^+$	Cm^r; *lacI*^{q}; P$_{T5\text{-}lac}$*ydgG*$^+$	1
pVS159	Amp^r; *qseB*::*lacZ* in pRS551	59
pVS176	Amp^r; *motA*::*lacZ* in pRS551	59
pVS175	Amp^r; *fliC*::*lacZ* in pRS551	59
pVS183	Amp^r; *fliAehK12*::*lacZ* in pRS551	59
pVS182	Amp^r; *flhD*::*lacZ* in pRS551	59
pLW11	Amp^r; *lsrACDBFG*::*lacZ* in pFZY1	65

[a] Amp^r, Km^r, Cm^r, and Em^r are ampicillin, kanamycin, chloramphenicol, and erythromycin resistance, respectively

(60). However, the means by which AI-2 is exported has not been identified, assuming that secretion of hydrophilic AI-2 requires active transport.

There are three studies describing *E. coli* global gene expression in biofilms (5, 48, 56). Beloin et al. (5) found biofilm cells have genes induced for stress response, cell biogenesis and transport, and energy and carbohydrate metabolism and that genes were repressed involving amino acid, carbohydrate, and inorganic ion transport; in all, 2% of all genes were differentially expressed more than twofold. Schembri et al. (56) found that 5% or 14% of the genes were differentially expressed compared to exponential- or stationary-phase suspended cultures, respectively. By comparing cells from the same reactor, we found that genes for stress response, type 1 fimbriae, and genes with unknown functions, including *ydgG* (*b1601*, 344 amino acids [aa]), are induced in biofilms after 7 h (48). The *ydgG* mutant was chosen for further study since this mutation increased biofilm formation upon addition of glucose to the medium.

To determine more rigorously the role of YdgG in biofilm formation, DNA microarrays were used here to study gene expression in a biofilm for a biofilm up mutant versus that of the isogenic wild-type strain. Previously, Zhu and Mekalanos (72) used microarrays to study genome expression in *V. cholerae* for a biofilm up mutant and found induced expression of *Vibrio* polysaccharide synthesis operons. We assumed that the differential gene expression of a poor biofilm-forming strain compared to its mutant that forms robust biofilms (e.g., *E. coli ydgG*) in a mature biofilm will show a wider view of the gene expression pattern in biofilm cells than an experiment that compares mature biofilm cells versus planktonic cells (33). Since many of the differentially expressed genes identified in the biofilm of the *ydgG* mutant are controlled by AI-2, we investigated the possibility that YdgG transports AI-2.

MATERIALS AND METHODS

Bacterial strains, plasmids, growth media, and growth rate measurements. The strains and plasmids used in this study are listed in Table 1. For *E. coli* K-12 BW25113 Δ*ydgG*, the insertion of the kanamycin resistance gene and the complete *ydgG* deletion were corroborated with five sets of PCRs (three primers homologous to sequences internal to the kanamycin gene and two primers homologous to a sequence upstream and downstream of *ydgG*) (1, 13). For plasmid selection, 100 μg/ml of ampicillin, 50 μg/ml of kanamycin, 30 μg/ml of chloramphenicol, or 300 μg/ml of erythromycin was added. Luria Bertani (LB) medium (55) was used for preculturing the *E. coli* strains. LM agar plates (18) were used for enumerating *V. harveyi* BB170, which was cultured in AB medium (3). For the 96-well biofilm assays, LB medium, LB medium supplemented with 0.2% glucose (LB glu), and M9 medium supplemented with 0.4% glucose and 0.4% Casamino Acids (M9C glu) (53) were used. M9C glu was also used for the *E. coli* flow cell experiment. The specific growth rates of wild-type and Δ*ydgG* strains were determined by measuring turbidity at 600 nm (optical density at 600 nm [OD$_{600}$]) and calculated by using the linear portion of the natural logarithm of OD$_{600}$ versus time (OD$_{600}$ from 0.05 to 0.5) in LB, LB glu, and M9C glu.

Ninety-six-well biofilm assay. The 96-well biofilm assay was conducted as described previously (52). Briefly, two independent overnight *E. coli* cultures were diluted to an OD$_{600}$ of 0.05 and grown in M9C glu, LB, or LB glu and the biofilms were stained with 0.1% crystal violet (Fisher, Hanover Park, IL) for 20 min to quantify the total biofilm mass (for both the biofilms at the bottom and those at the air-liquid interface). Each datum point was averaged from two independent experiments, each with four replicate wells.

Flow cell biofilm experiments and image analysis. M9C glu supplemented with 300 μg/ml erythromycin to maintain constitutive green fluorescent protein plas-

mid pCM18 (22) was used to form biofilms at 37°C in a continuous-flow cell as described previously (19). The biofilm was visualized at 24 h with a TCS SP2 scanning confocal laser microscope (Leica Microsystems, Heidelberg, Germany) with a 40× N PLAN L dry objective with a correction collar and a numerical aperture of 0.55. Color confocal flow cell images were analyzed with COMSTAT image-processing software (24) as described previously (52). At 24 h, nine different positions were chosen for microscope analysis and 25 images were processed for each position; in total, 225 images were analyzed. The values reported are means of data from the different positions at the same time point, and standard deviations were calculated based on these mean values for each position. Simulated three-dimensional images were obtained with IMARIS (BITplane, Zurich, Switzerland). Twenty-five pictures were processed for each three-dimensional image.

Motility assay. The motility assay was adapted from Sperandio et al. (59); LB overnight cultures were used to assay motility in plates containing 1% (wt/vol) tryptone, 0.25% (wt/vol) NaCl, and 0.3% (wt/vol) agar (where indicated, motility plates were supplemented with glucose or chloramphenicol). Motility halos were measured at 16 h, and five to eight plates were used to compare motility between the strains. For the motility complementation experiment, motility ratios between the *ydgG* mutant and the wild-type strain are used in order to eliminate the small density differences between the motility plates. On each plate, both the wild type and the *ydgG* mutant were inoculated.

Promoter transcriptional assays. *E. coli* cultures with plasmids containing the *flhD*::*lacZ*, *fliA*::*lacZ*, *fliC*::*lacZ*, *motA*::*lacZ*, and *qseB*::*lacZ* fusions (Table 1) were cultured overnight in LB medium supplemented with ampicillin (100 μg/ml) and then diluted 1:100 in LB and LB glu (both supplemented with 100 μg/ml ampicillin) to create exponentially growing cells that were harvested at an OD_{600} of 1. β-Galactosidase activity was assayed as described previously (68). All activities were calculated based on a protein concentration of 0.24 mg protein/ml/OD_{600} unit. Each experiment was performed twice with two different cultures for each strain in LB and LB glu.

Complementation of motility, biofilm, drug resistance, and extracellular AI-2 phenotypes. The *ydgG* deletion was complemented in *trans* with pCA24N *ydgG*$^+$ (1, 13), which has isopropyl-β-D-thiogalactopyranoside (IPTG; Sigma, St. Louis)-inducible expression of *ydgG*$^+$. Control of *ydgG*$^+$ transcription was tight due to the presence of *lacI*^{q}. The same plasmid without the *ydgG*$^+$ insertion, pCA24N, was used as a negative control. Overnight cultures with IPTG (0, 0.5, 0.75, 1.0, and 1.5 mM) were used for the 96-well biofilm assay, motility assay, drug resistance assay, and extracellular AI-2 activity assay. Chloramphenicol (30 μg/ml) was added to the growth media and motility agar, except for the 96-well assay, where 50 μg/ml chloramphenicol was used in the biofilm assay. For complementing the extracellular AI-2 activity, cells were harvested at an OD_{600} of 0.6, washed twice (10 min at 8,820 × *g*) to remove chloramphenicol (inhibits the growth of the *Vibrio* reporter), and resuspended in the same volume of 20 ml LB glu. Then cells were grown to an OD_{600} of 0.9 for AI-2 production in the absence of chloramphenicol.

AI-2 assays. To determine extracellular AI-2 concentrations, overnight *E. coli* cultures were diluted 1:100 and grown to exponential phase (OD_{600} of 0.6) in LB and LB glu. Filter-sterilized supernatants were prepared and assayed as described previously with the reporter *V. harveyi* BB170 (51). To determine the intracellular AI-2 concentration, overnight cultures of *E. coli* containing *lsrACDBFG*::*lacZ* (Table 1) were diluted to create both exponentially growing and stationary-phase cells and so were harvested at OD_{600} values of 0.6 and 6, respectively, and then β-galactosidase activity was assayed as described previously (68). Taga et al. (62) showed that as AI-2 is internalized, higher β-galactosidase activity is measured from the *lsr*::*lacZ* fusion.

Drug transport measurements. Analysis of the effect of the *ydgG* mutation on the MICs of various antibiotics was conducted as described previously (35). Briefly, strains were grown overnight in LB glu and for the *ydgG* mutant, the medium was supplemented with 50 μg/ml kanamycin. The overnight culture was diluted 1:100 in LB glu, grown to an OD_{600} of 0.4, and cooled to 4°C. The cells were grown again, after dilution of the cultures (OD_{600} of 0.4) to a cell density of 5×10^4 cells/ml in LB glu with 50- to 500-fold increasing concentrations of drugs (streptomycin sulfate and spectinomycin at 1 to 50 μg/ml, crystal violet at 10 to 500 μg/ml, chloramphenicol at 0.1 to 10 μg/ml, amoxicillin at 0.1 to 10 μg/ml, 2,6-dichloroquinone-4-chloroimide at 5 to 500 μg/ml, penicillin G at 1 to 500 μg/ml, erythromycin at 5 to 500 μg/ml, sodium dodecyl sulfate at 10 to 1,000 μg/ml, ampicillin at 0.1 to 10 μg/ml, and tetracycline at 0.1 to 10 μg/ml). The OD_{600} was measured after 18 h of incubation at 250 rpm at 37°C.

Biofilm total RNA isolation for DNA microarrays. Overnight cultures were diluted 100-fold into 1-liter shake flasks containing 250 ml of LB glu and 10 g of glass wool. The cells were shaken at 250 rpm at 37°C for 24 h (final OD_{600} of 5 for the suspended cells) to form a biofilm on the glass wool, and RNA was isolated from the biofilm as described previously (48).

DNA microarrays. The *E. coli* GeneChip antisense genome array (P/N 900381; Affymetrix) was used to study the differential gene expression profile of the *ydgG* mutant compared to that of the isogenic wild type in a mature biofilm as described in the *Gene Expression Technical Manual* and as previously published (19). The data were inspected for quality and analyzed as described in *Data Analysis Fundamentals*, which includes using premixed polyadenylated transcripts of the *B. subtilis* genes (*lys*, *phe*, *thr*, and *dap*) at different concentrations. Also, as expected, there was insignificant *ydgG* mRNA signal in the biofilm of the *ydgG* mutant (60-fold lower than the mean signal and 13-fold lower than the signal accepted from the *ydgG* open reading frame [ORF] in the wild-type strain), and the genes which are known to be completely deleted from *E. coli* K-12 BW25113 (e.g., *araA* and *rhaA*) showed insignificant mRNA levels. To ensure the reliability of the induced-repressed gene list, genes were identified as differentially expressed if the *P* value was less than 0.05 and if the expression ratio was greater than 2 since the standard deviation for the expression ratio for all the genes was 2.2 (GEO accession number GSE3514). The gene functions were obtained from the National Center for Biotechnology Information database (http://www.ncbi.nlm.nih.gov/); the Institute for Genomic Research, University of California at San Diego; and the UNAM database (http://biocyc.org/ECOLI/).

RESULTS

YdgG represses biofilm formation without affecting growth. Almost no change in the growth rate was observed when *ydgG* was deleted from *E. coli* K-12; the growth rates in LB medium were 1.49 ± 0.05 versus 1.67 ± 0.05/h, in LB glu they were 1.73 ± 0.0 versus 1.80 ± 0.02/h, and in M9C glu they were 1.01 ± 0.01 versus 1.15 ± 0.03/h for the wild-type strain and the *ydgG* mutant, respectively. However, this deletion increased biofilm formation in 96-well plates when glucose was added to the medium (3.8-fold ± 0.2-fold for LB glu and 1.6-fold ± 0.1-fold for M9C glu) and decreased biofilm formation for LB medium (0.5-fold ± 0.1-fold).

The increase in biofilm formation in M9C glu measured by the crystal violet assay was corroborated in the more rigorous continuous-flow system, where the *ydgG* deletion dramatically increased biofilm formation (Fig. 1). The wild-type biofilm architecture in the flow cell consists of only a few individual cells on less than 1% of the observable surface, while the *ydgG* mutant formed a flat biofilm covering at least 30% of the viewable area and was composed of large, irregularly shaped, smooth masses containing random protrusions (Fig. 1). These changes in biofilm architecture were quantified with the COMSTAT computer program for quantifying biofilm structures (24); compared to the wild type, after 24 h, the biomass increased 574-fold, the substratum coverage increased 10-fold, the mean thickness was increased 7,000-fold, and the roughness coefficient was decreased 12-fold. Although different biofilm systems were used to measure the effect of YdgG on biofilm formation (one involves static conditions, and the other involves flow), an enhancement of biofilm formation with the *ydgG* mutant was obtained consistently and the difference in biofilm formation between the two systems may be attributed to the differences in the biofilm assays.

To confirm that the increase in biofilm formation is due to the deletion of *ydgG*, the mutant strain was complemented in *trans* and biofilm formation was measured in a 96-well biofilm assay with M9C glu and LB glu. As expected, increasing *ydgG* expression decreased the biofilm formation of the *ydgG* mutant in both M9C glu and LB glu to that of the wild-type strain. In M9C glu, at IPTG concentrations of 0.5, 0.75, 1.0, and 1.5 mM, the relative values of biofilm formation by the *ydgG* mutant

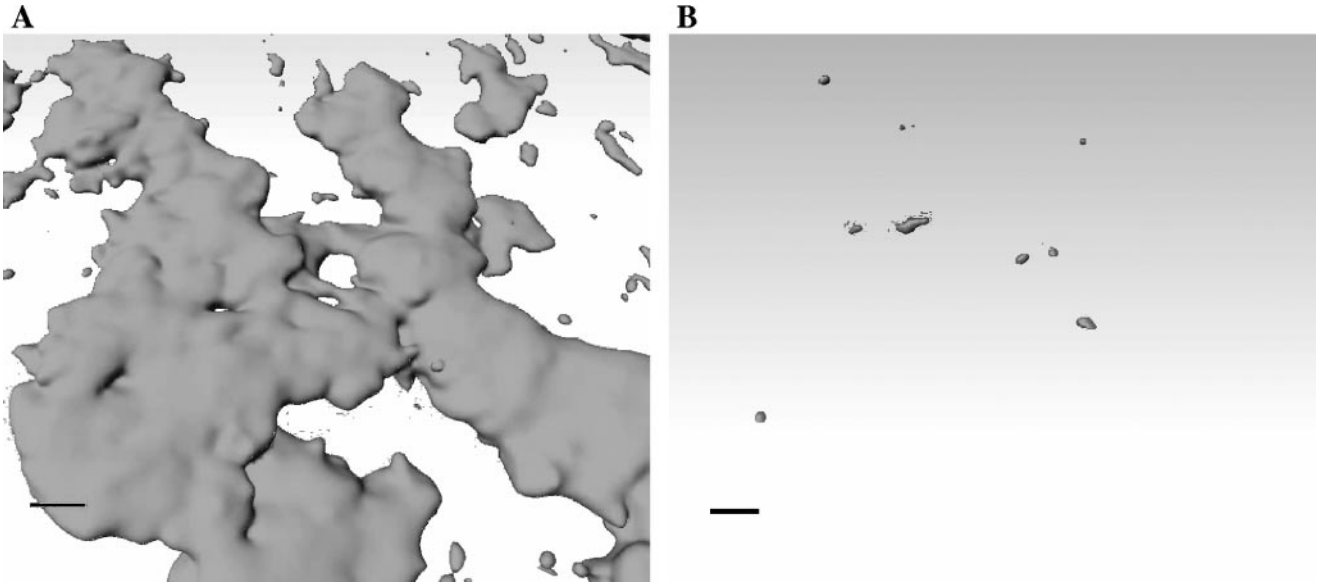

FIG. 1. Effect of *ydgG* deletion (A) on biofilm formation in a flow chamber with M9C glu versus wild-type *E. coli* (B). Biomass was measured after 24 h, and images were analyzed with IMARIS. Scale bars, 10 μm.

expressing YdgG in *trans* were 1.9 ± 0.3, 1.8 ± 0.3, 1.1 ± 0.2, and 1.1 ± 0.2, respectively. In LB glu, at the same IPTG concentrations, the relative values of biofilm formation by the *ydgG* mutant expressing YdgG in *trans* were 1.8 ± 0.2, 1.6 ± 0.2, 1.4 ± 0.2, and 0.9 ± 0.2, respectively. Hence, YdgG represses biofilm formation.

YdgG represses motility. Compared to the wild-type strain, deletion of *ydgG* resulted in a sixfold increase in swimming motility; the motility diameter for the wild-type strain was 0.3 ± 0.2 cm versus 2.0 ± 0.5 cm for the *ydgG* mutant (there was no effect of glucose). Similar to complementing biofilm formation, as *ydgG*$^+$ was induced in *trans*, the motility of *E. coli* Δ*ydgG*/pCA24N *ydgG*$^+$ became equal to that of the wild-type strain containing plasmid pCA24N, indicating the motility phenotype could be complemented. At IPTG concentrations of 0.1, 0.25, 0.5, 0.75, and 1.0 mM, the relative values for the motility of the *ydgG* mutant expressing YdgG in *trans* were 3.8 ± 0.2, 3.4 ± 0.1, 1.8 ± 0.1, 1.6 ± 0.0, and 1.0 ± 0.1, respectively. Hence, YdgG represses motility.

To determine the cause of this increase in motility seen upon deletion of *ydgG*, transcription of the quorum-sensing response regulator of flagellum genes (*qseB*), flagellar synthesis genes (*flhD*, *fliA*, and *fliC*), and the motility gene (*motA*) was investigated. The *ydgG* mutation increased the expression of these flagellum and motility genes 15- to 120-fold in both LB and LB glu (Fig. 2).

YdgG increases extracellular AI-2 activity. Significantly higher extracellular AI-2 activity was measured for the wild-type strain compared to the *ydgG* mutant in both LB (13-fold ± 9-fold) and LB glu (4-fold ± 2-fold) under exponential growth conditions (relative light units measured per cell of *V. harveyi* BB170 were $(3.4 \pm 0.6) \times 10^{-5}$ and $(8.0 \pm 0.1) \times 10^{-5}$ for the wild-type strain, respectively). Hence, YdgG appears to have a role in either enhancing AI-2 export from the cell or inhibition of AI-2 uptake. As expected (60), extracellular AI-2 activity was higher for both the wild type and the *ydgG* mutant

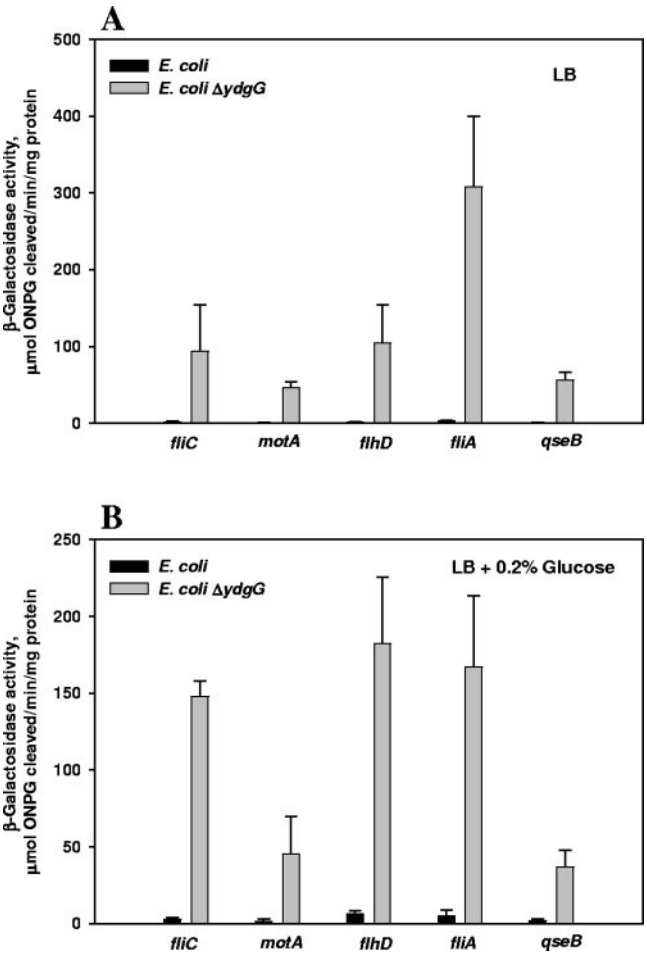

FIG. 2. Effect of deletion of *ydgG* on the transcription of *flhD*, *fliA*, *fliC*, *motA*, and *qseB* in LB (A) and LB glu (B) for cells in suspension. The experiment was done in duplicate, and 1 standard deviation is shown. ONPG, *o*-nitrophenyl-β-D-galactopyranoside.

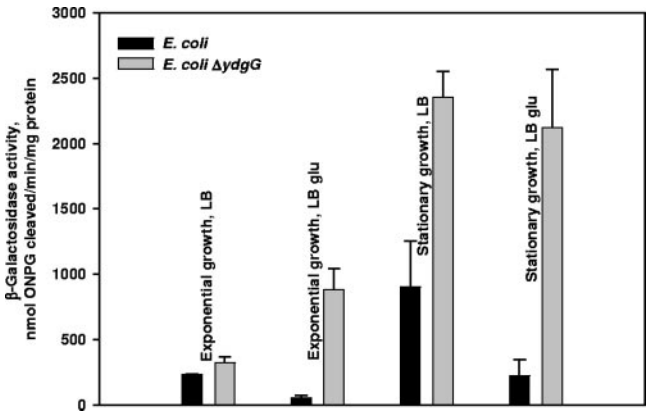

FIG. 3. Effect of deletion of *ydgG* on transcription of the *lsrACDBFG* operon with exponentially growing and stationary-phase cells in suspension in LB and LB glu. The experiment was done in duplicate, and 1 standard deviation is shown. ONPG, *o*-nitrophenyl-β-D-galactopyranoside.

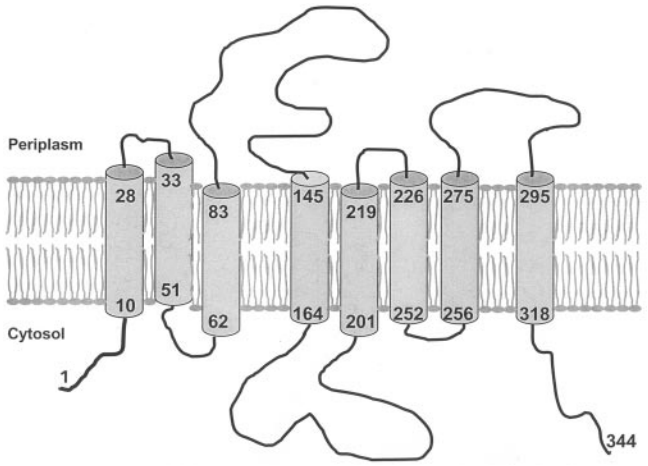

FIG. 4. Schematic of YdgG combining data predicted by different bioinformatic programs.

upon the addition of glucose to LB medium (2-fold ± 0.5-fold and 7-fold ± 5-fold, respectively).

Similar to complementing biofilm formation and motility, by expressing *ydgG*$^+$ in *trans*, we were able to increase the extracellular AI-2 activity of the *E. coli ydgG* mutant to that of the wild-type strain (containing control plasmid pCA24N) by expressing *ydgG*$^+$ in *trans* in LB glu with pCA24N *ydgG*$^+$. At IPTG concentrations of 0.5, 0.75, 1.0, and 1.5 mM, the relative extracellular AI-2 concentrations of the *ydgG* mutant expressing YdgG in *trans* were 0.3 ± 0.3, 0.5 ± 0.4, 0.8 ± 0.2, and 1.0 ± 0.3, respectively.

YdgG reduces intracellular AI-2 activity. Significantly higher intracellular AI-2 activity was measured for the *ydgG* mutant compared to the wild-type strain in LB glu (16-fold ± 5-fold and 10-fold ± 5-fold under exponential-growth and stationary-phase conditions, respectively) (Fig. 3), as determined by comparing transcription of the *lsrACDBFG* promoter region. This operon is induced by internal phosphorylated AI-2 produced by the cytoplasmic kinase LsrK and intracellular AI-2 (62). Hence, once again, YdgG appears to either enhance AI-2 export from the cell or inhibit AI-2 uptake. As expected, addition of glucose to the wild-type strain repressed *lsr* transcription via catabolic repression by 4.0-fold ± 0.3-fold and 4.0-fold ± 0.7-fold during the exponential and stationary phases, respectively (65). Since transport of AI-2 is altered in the *ydgG* mutant, addition of glucose had no effect on the *ydgG* mutant during stationary phase (Fig. 3); some increase (2.7-fold ± 0.3-fold) in the intracellular AI-2 concentration was observed upon glucose addition during exponential growth of the *ydgG* mutant (Fig. 3). Future experiments with a *luxS ydgG* double mutant should be performed to investigate whether the *ydgG* mutation affects *lsr* expression.

YdgG increases drug susceptibility. If YdgG is a transporter, one might expect it to affect drug resistance (27); hence, we tested the impact of the *ydgG* deletion with 11 different antimicrobials. Higher resistance of the *ydgG* mutant was observed with the following drugs compared to the wild-type strain: crystal violet (MICs of 100 and 250 μg/ml, respectively), spectinomycin (MICs of 20 and 50 μg/ml, respectively), streptomycin sulfate (MICs of 5 and 10 μg/ml, respectively), 2,6-dichloroquinone-4-chloroimide (MICs of 50 and 100 μg/ml, respectively), chloramphenicol (MICs of 5 and 10 μg/ml, respectively), and amoxicillin (MICs of 5 and 10 μg/ml, respectively). No change in resistance to the other drugs used was observed. Also, when expressing *ydgG* in *trans* in the *ydgG* mutant with pCA24N *ydgG*$^+$, the phenotype could be complemented in that a higher susceptibility to crystal violet was observed in the mutant as the IPTG concentration was increased; BW25113 Δ*ydgG*/pCA24N *ydgG*$^+$ grew to an OD_{600} of 0.9 after 18 h in LB glu supplemented with 30 μg/ml chloramphenicol, but addition of 0.5 mM IPTG caused no growth (no growth was observed in the controls BW25113/pCA24N and BW25113/pCA24N *ydgG*$^+$).

Prediction of YdgG structure and function. Multiple secondary-structure prediction programs, such as PSIPRED (38), JPRED (10), and PHD (54), were used to identify the secondary structure of YdgG as almost exclusively all α-helical. Additionally, a ProDom (7) and BLAST (37) search indicated that YdgG most likely functions as a transporter and is predicted to be a membrane protein. Therefore, the membrane protein topology prediction programs MEMSTAT-2 (25, 26), TMHMM (31, 57), and PHDhtm (54) were used to predict seven to eight transmembrane helices, and the topology of the α-helices is shown in Fig. 4. The results from these programs correlated very well, and all predict (with 50 to 75% reliability) that the first loop is out of the membrane and the N and the C termini are cytosolic. Between residues 83 and 145 and residues 164 and 201, large loops are predicted, which could potentially play a role in regulating the transport of YdgG.

Differential gene expression in biofilms due to deletion of *ydgG*. To explore further the mechanism by which YdgG represses biofilms, differential gene expression in the biofilms (rather than in suspension) as a result of deletion of *ydgG* was investigated; it was found that 1,330 (31%) of the *E. coli* genes were differentially induced and 327 (8%) were differentially repressed when a twofold cutoff was used (292 genes were induced and 99 genes were differentially repressed when a threefold cutoff was used). The most significantly induced and

repressed genes (more than fourfold) are summarized in Tables 2 and 3.

Deletion of *ydgG* increased AI-2 intracellular activity during both the exponential and stationary phases in shake flasks (Fig. 3); hence, many genes that are induced by AI-2 synthesis via active LuxS (49, 58) were induced in the *ydgG* mutant. For example, 87% of the genes induced by AI-2 (49) were also induced here in the biofilm culture of the *ydgG* mutant more than 1.5-fold, and 41% of AI-2-repressed genes (49) were repressed here more than 1.5-fold in the biofilm of the *ydgG* mutant. Also, 94% of the flagellum and motility genes reported to be induced by AI-2 by Sperandio et al. (58) were induced in the biofilm of the *ydgG* mutant (1.5-fold cutoff), and 70% of the differentially expressed genes in the study of Sperandio et al., which are involved in growth and cell division, showed the same expression (induced and repressed more than 1.5-fold) in the biofilm of the *ydgG* mutant.

The most significantly induced genes in the biofilm due to deletion of *ydgG* are those related to the cell envelope, transport, polysialic acid production, phage functions, methionine biosynthesis, biotin and thiamine biosynthesis, anaerobic metabolism, and unknown function (Table 2). The most significant cell envelope transport genes induced were *acrEF* (24- and 5.7-fold). AcrEF is a multidrug efflux system in *E. coli* which secretes indole, the product of tryptophan degradation (27). Indole was found to act as an extracellular signal in *E. coli* and to regulate biofilm formation (16) and amino acid degradation (64). An unknown stationary-phase signal has been found previously that is related to indole (50, 64). This stationary-phase signal was found to repress AI-2 extracellular activity and to induce genes related to biofilm formation such as *fliK*, *tnaA*, and *ybaJ* (50).

Genes involved in biofilm formation (43) were found to be induced due to *ydgG* deletion. For example, the four operons for flagellar synthesis (8) were induced in the *ydgG* mutant biofilm. The class 1 master flagellar regulator *flhC* was induced 2.1-fold, which led to overexpression of *flhDC*-induced class 2 flagellum genes, including the *flgABCDEFGHIJ* operon, where the most significant increase in expression was observed in *flgI* (induced 6.5-fold). Other class 2 flagellum operons were also induced in the *ydgG* mutant, including *flhA* and *flhB* (both induced twofold). The *fliEFGHIJK* operon was also induced 2.5-fold, and *fliLMNOPQR* was induced 2.1- to 3.2-fold. The sigma factor FliA, σ^{28}, was induced 2.1-fold (activates class 3 flagellum operons [8]), and the force generator gene *motA* and its motility and chemotaxis operon (*motAB* and *cheAW*) were induced around twofold. The chemotactic response gene *cheZ* was also induced 2.5-fold. *fliD* (encoding the filament cap FliD) was induced 2.5-fold. *fliS* and *fliT* encoding FliD chaperones were both induced 2.1-fold. Other class 3 flagellum genes were also induced; *flgN*, encoding the hook-filament chaperone proteins FlgK and FlgL, was induced 2.3-fold. The lower relative induction of the flagellum genes in the biofilms of the *ydgG* mutant (determined via microarrays) compared to the induction of flagellum genes observed in the exponential-phase suspension cultures of the *ydgG* mutant (Fig. 2) may be attributed to the two different modes of bacterial growth.

Adhesion determinants induced in the *ydgG* biofilm include the type 1 fimbria operon, other putative type 1 fimbria operons, and Ag43. Type 1 fimbriae are an important determinant of *E. coli* adhesion to both biotic and abiotic surfaces (43) during the first step of cell attachment to a surface. In the *ydgG* biofilm, *fimB* and *fimE* were induced 2.6- and 2-fold, respectively. Another eight putative type 1 fimbria-like predictive operons (http://biocyc.org/ECOLI/) were induced, with at least two genes from each operon induced more than twofold. The most highly induced was the *sfm* gene cluster, where *sfmD*, encoding a putative outer membrane protein, was induced fourfold. *fimZ*, an activator of FimA (located in the *sfm* gene cluster, which is involved in type 1 fimbria gene expression) (71), was also induced fourfold. The surface adhesin autotransporter protein Ag43 (encoded by *flu*) was induced 2.5-fold and is also known to promote biofilm formation (29). The two curli production operons in charge of producing the major (CsgA) and minor (CsgB) subunits of these fibronectin tentacle filaments were induced; *csgBAC* was induced 2.1- to 2.5-fold, and *csgDEFG* was induced 2- to 4-fold. Curli fibers are required both for adhesion and biofilm maturation (44). Also, the *pgaABCD* operon was induced 2- to 2.8-fold; this operon produces the β-1,6-*N*-acetyl-D-glucosamine polysaccharide adhesin, which affects biofilm formation (66).

The colanic acid operon (*wza wzb wzc wcaABCDEFG*), involved in polysaccharide production, was induced (two- to sevenfold) when the highest expression ratio was observed in *wcaC*, a putative glycosyltransferase. Colanic acid is important for biofilm three-dimensional structure rather than the initial attachment of cells to a surface (44).

Other induced genes in the *ydgG* biofilm include those which encode uncharacterized proteins, including *yihR* (11-fold, putative aldose-1-epimerase), *yihN* (12-fold, putative proton-driven sugar phosphate uptake protein), *yihP* (11-fold, putative transport protein for galactosides-pentoses-hexuronides), and *yfjR* (16-fold, putative protein related to phage).

Biofilm formation after deletion of the 15 most significantly induced genes. To investigate the genes which may affect biofilm formation, 15 isogenic *E. coli* K-12 strains with mutations in the highly induced genes were assayed for biofilm formation after 24 h of growth in the 96-well biofilm assay. As expected, 14 of the 15 had reduced biofilm formation and 10 out of the 15 mutations resulted in 40% or more biofilm removal (Fig. 5). Deletion of the gene that encodes YfjR, a putative transcriptional repressor probably related to phage, showed the largest decrease in biofilm formation (65%). Other genes which affect biofilm formation were a biotin synthesis-related gene (*bioF*), a gene that encodes a putative methyltransferase (*yccW*), genes that encode putative regulatory proteins with an unknown function (*yjbE* and *yceO*), genes related to anaerobic metabolism (*ttdA* and *fumB*), a gene that encodes an uncharacterized protein (*yjiP*, probably transposon related), a gene that encodes a putative aldose-1-epimerase (*yihR*), and a polysialic acid production-related gene (*gutQ*). The *acrE* deletion did not seem to affect biofilm formation after 24 h of growth, which is probably due to AcrAB complementing AcrEF (30). Therefore, 10 genes (*yfjR*, *bioF*, *yccW*, *yjbE*, *yceO*, *ttdA*, *fumB*, *yjiP*, *gutQ*, and *yihR*) that were not previously linked with biofilms were shown here to be involved in biofilm formation, including 1 that suggests a role for polysialic acid (via *gutQ*) in *E. coli* biofilms.

TABLE 2. Genes induced more than fourfold in LB glu medium biofilms upon deleting *ydgG*

Group and gene	b no.	Expression ratio	Description	Protein size (aa)
Synthesis and metabolism				
bioF	*b0776*	21.1	8-Amino-7-oxononanoate synthase	384
pflD	*b3951*	13.9	Formate acetyltransferase 2	765
yfdW	*b2374*	12.1	Putative enzyme; formyl-CoA[a] transferase monomer, subunit of formyl-CoA transferase	416
citG	*b0613*	12.1	ORF, hypothetical protein; triphosphoribosyl-dephospho-CoA synthase	292
yihR	*b3879*	11.3	Putative aldose-1-epimerase	308
ttdA	*b3061*	11.3	L-Tartrate dehydratase, subunit A	303
nth	*b1633*	10.6	Endonuclease III, specific for apurinic and/or apyrimidinic sites	211
gutM	*b2706*	9.8	Glucitol operon activator	119
eutA	*b2451*	9.8	Reactivating factor for ethanolamine ammonia lyase EutBC	467
gutQ	*b2708*	9.2	ORF, hypothetical protein; protein with a sugar isomerase domain; GutQ has similarity to *E. coli* K1	308
fumB	*b4122*	9.2	Fumarase B fumarate hydratase class I; anaerobic isozyme	548
yieL	*b3719*	8.6	Putative xylanase	400
yagH	*b0271*	8	Putative beta-xylosidase	536
thiD	*b2103*	8	Phosphomethylpyrimidine kinase (thiamine biosynthesis)	266
mhpB	*b0348*	7.5	2,3-Dihydroxyphenylpropionate 1,2-dioxygenase	314
wcaC	*b2057*	7	Putative glycosyl transferase; colanic acid related	405
thiF	*b3992*	7	Thiamine-biosynthesis, thiazole moiety	245
napA	*b2206*	7	Probable nitrate reductase 3	832
ybjW	*b0873*	6.5	Putative prismane; hybrid cluster protein/hydroxylamine reductase	552
hyfD	*b2484*	6.5	Hydrogenase 4 membrane subunit	479
hyfA	*b2481*	6.5	Hydrogenase 4 Fe-S subunit	205
purC	*b2476*	6.1	Phosphoribosylaminoimidazole-succinocarboxamide synthetase, SAICAR synthetase	237
citC	*b0618*	6.1	Citrate lyase synthetase (citrate [pro-3S]-lyase ligase)	381
wcaA	*b2059*	5.7	Putative regulator for colanic acid synthesis	279
lysA	*b2838*	5.3	Diaminopimelate decarboxylase	420
abgB	*b1337*	5.3	ORF, hypothetical protein; member of the GMP family of beta barrel pores	481
treC	*b4239*	4.9	Trehalase 6-P hydrolase	551
arp	*b4017*	4.9	Regulator of acetyl-CoA synthetase	728
argF	*b0273*	4.9	Ornithine carbamoyltransferase 2, chain F (arginine biosynthesis)	334
metR	*b3828*	4.6	Regulator for *metE* and *metH*, homocysteine transcriptional activator	348
agaW	*b3134*	4.6	Phosphotransferase system *N*-acetylgalactosameine-specific IIC component 2	133
ygbD	*b2711*	4.3	Putative oxidoreductase; reductase enzyme which can convert oxidized flavorubredoxin to its reduced form (NO removal)	377
torT	*b0994*	4.3	Part of regulation of *tor* operon, periplasmic	342
hybC	*b2994*	4.3	Probable large subunit, hydrogenade 2	567
Metabolism and transport				
wza	*b2062*	4	Putative polysaccharide export protein	379
Transport				
yccW	*b0967*	17.1	Putative oxidoreductase; putative methyltransferase	367
focB	*b2492*	13.9	Probable formate transporter (formate channel 2); FocB formate FNT[b] transporter	282
yihN	*b3874*	12.1	Putative resistance protein (transport)	421
yjhQ	*b4307*	11.3	ORF, hypothetical protein	181
yihP	*b3877*	10.6	Putative permease	468
uraA	*b2497*	8.6	Uracil transport	429
yhfM	*b3370*	7.5	Putative amino acid/amine transport protein; YhfM methionine APC[c] transporter	462
dcuB	*b4123*	6.5	Anaerobic dicarboxylate transport	446
malK	*b4035*	6.1	ATP-binding component of transport system for maltose	371
acrF	*b3266*	5.7	Integral transmembrane protein; acridine resistance	1,034
artJ	*b0860*	5.3	Arginine 3rd transport system periplasmic binding protein	243
pheP	*b0576*	4.9	Phenylalanine-specific transport system	458
ycfT	*b1115*	4.3	ORF, hypothetical protein; putative transport protein	357
agaD	*b3140*	4	Phosphotransferase system, *N*-acetylglucosamine enzyme IID component 1	263
Structure				
acrE	*b3265*	24.3	Transmembrane protein affects septum formation and cell membrane permeability	385
flgI	*b1080*	6.5	Homolog of *Salmonella* P ring of flagellar basal body	365
uhpB	*b3668*	4.6	Sensor histidine protein kinase phosphorylates UhpA	501
fhiA	*b0229*	4.3	Flagellar biosynthesis	579

Continued on following page

TABLE 2—*Continued*

Group and gene	b no.	Expression ratio	Description	Protein size (aa)
sfmD	*b0532*	4	Putative outer membrane protein, export function; sequence similarity suggests that it is a member of the fimbrial usher protein family	867
hyfC	*b2483*	4	Hydrogenase 4 membrane subunit	322
csgE	*b1039*	4	Curli production assembly/transport component, second curli operon	129
RNA related				
ybcJ	*b0528*	17.1	ORF, hypothetical protein; putative RNA-binding protein	77
envR	*b3264*	4.9	Putative transcriptional regulator	220
hycA	*b2725*	4	Transcriptional repression of *hyc* and *hyp* operons; involved in the formate hydrogenylase system	153
fimZ	*b0535*	4	Fimbrial Z protein; probable signal transducer; positive DNA-binding transcriptional regulator	210
Phage related				
alpA	*b2624*	6.5	Prophage CP4-57 regulatory protein AlpA	70
intE	*b1140*	4.6	Prophage e14 intergrase	375
cspB	*b1557*	4.6	Cold shock protein; may affect transcription; transcriptional regulator	71
stfE	*b1157*	4	Putative tail fiber protein	179
Cell processes				
ampC	*b4150*	4.3	β-Lactamase; penicillin resistance	377
pphB	*b2734*	4	Protein phosphatase 2	218
ibpB	*b3686*	4	Heat shock protein	144
ORFs with unknown function				
yjiP	*b4338*	19.7	ORF, hypothetical protein	103
yghG	*b2971*	18.4	ORF, hypothetical protein	655
yfjR	*b2634*	16	ORF, hypothetical protein; putative transcriptional repressor, probably related to phage	233
ybfG	*b0690*	12.1	ORF, hypothetical protein	120
yceO	*b1058*	11.3	ORF, hypothetical protein	46
yafX	*b0248*	11.3	ORF, hypothetical protein	152
ylbE	*b0519*	8.6	ORF, hypothetical protein	333
yjbE	*b4026*	7.5	ORF, hypothetical protein	80
ves	*b1742*	7.5	ORF, hypothetical protein; cold-induced member of CspA family	212
ybfP	*b0689*	7	Putative pectinase	164
yjgI	*b4249*	6.1	Putative oxidoreductase	237
ybfE	*b0685*	6.1	ORF, hypothetical protein; LexA regulated	120
yijI	*b3948*	5.3	ORF, hypothetical protein	27
yjbL	*b4047*	4.9	ORF, hypothetical protein	84
yddJ	*b1470*	4.9	ORF, hypothetical protein	111
ybjI	*b0844*	4.9	ORF, hypothetical protein; conserved protein with phophatase-like domain	262
yjfM	*b4185*	4.6	ORF, hypothetical protein	212
yecT	*b1877*	4.6	ORF, hypothetical protein	169
ybhM	*b0787*	4.6	ORF, hypothetical protein	237
b0309	*b0309*	4.6	ORF, hypothetical protein	70
b1500	*b1500*	4.3	ORF, hypothetical protein; gene is in an operon associated with acid resistance	65
b1228	*b1228*	4.3	ORF, hypothetical protein	91
ytfA	*b4205*	4	ORF, hypothetical protein	108
yoaG	*b1796*	4	ORF, hypothetical protein	60
yjgN	*b4257*	4	ORF, hypothetical protein; putative membrane protein possibly involved in transport	398
yjcF	*b4066*	4	ORF, hypothetical protein	430
yhaC	*b3121*	4	ORF, hypothetical protein	395
ygfF	*b2902*	4	Putative oxidoreductase	247
yfdU	*b2373*	4	Putative enzyme	564
yfaE	*b2236*	4	ORF, hypothetical protein; conserved hypothetical protein, related to 2Fe-2S ferredoxin	84
yfaA	*b2230*	4	ORF, hypothetical protein	578
yadS	*b0157*	4	ORF, hypothetical protein	207
b0370	*b0370*	4	ORF, hypothetical protein	89

[a] CoA, coenzyme A.
[b] FNT, formate and nitrate transporter family.
[c] APC, amino acid-polyamine-organocation.

TABLE 3. Genes repressed more than fourfold in LB glu medium biofilms upon deleting *ydgG*

Group and gene	b no.	Expression ratio	Description	Protein size (aa)
Synthesis and metabolism				
gadA	*b3517*	−13	Glutamate decarboxylase isozyme	466
gadB	*b1493*	−10.6	Glutamate decarboxylase isozyme	466
aceA	*b4015*	−5.7	Isocitrate lyase	434
fadB	*b3846*	−4.9	Four-enzyme protein: 3-hydroxyacyl-CoA[a] dehydrogenase, 3-hydroxybutyryl-CoA epimerase, delta(3)-*cis*-delta(2)-*trans*-enoyl-CoA isomerase, enoyl-CoA hydratase	729
nrdH	*b2673*	−4.6	Glutaredoxin-like protein; hydrogen donor	81
thrL	*b0001*	−4.3	*thr* operon leader peptide	21
Metabolism and transport				
fadL	*b2344*	−6.1	Transport of long-chain fatty acids; sensitivity to phage T2	448
Transport				
gadC (xasA)	*b1492*	−11.3	Acid sensitivity protein, putative transporter	512
dppA	*b3544*	−7	Dipeptide transport protein	535
DNA related				
priB	*b4201*	−4.9	Primosomal replication protein N	104
tsf	*b0170*	−4	Protein chain clongation factor EF-Ts	283
RNA related				
rpoE	*b2573*	−4.9	RNA polymerase, sigma-E factor; heat shock and oxidative stress	191
leuT	*b3798*	−4.6	Leucine tRNA1, duplicate with *leuVPO*	87
leuV	*b4368*	−4.6	Leucine tRNA1, tandemly triplicate *leuVPQ*, duplicate with *leuT*	88
thrT	*b3979*	−4.6	Threonine tRNA3	76
leuP	*b4369*	−4	Leucine tRNA1, tandemly triplicate *leuVPO*, duplicate with *leuT*	87
leuQ	*b4370*	−4	Leucine tRNA1, tandemly triplicate, duplicate with *leuT*	87
Ribosome components				
rplC	*b3320*	−8.6	50S ribosomal subunit protein L3	209
rplB	*b3317*	−8	50S ribosomal subunit protein L2	273
rplW	*b3318*	−7.5	50S ribosomal subunit protein L23	100
rpsJ	*b3321*	−7.5	30S ribosomal subunit protein S10	103
rpsS	*b3316*	−7.5	30S ribosomal subunit protein S19	92
rplD	*b3319*	−6.1	50S ribosomal subunit protein L4; regulates expression of S10 operon	201
rplV	*b3315*	−6.1	50S ribosomal subunit protein L22	110
rpsC	*b3314*	−6.1	30S ribosomal subunit protein S3	233
rpmB	*b3637*	−5.3	50S ribosomal subunit protein L28	78
rpsB	*b0169*	−5.3	30S ribosomal subunit protein S2	241
rpsF	*b4200*	−5.3	30S ribosomal subunit protein S6	131
rplU	*b3186*	−4.9	50S ribosomal subunit protein L21	103
rpsR	*b4202*	−4.9	30S ribosomal subunit protein S18	75
rpmG	*b3636*	−4.6	50S ribosomal subunit protein L33	55
rplK	*b3983*	−4.3	50S ribosomal subunit protein L11	142
rplP	*b3313*	−4	50S ribosomal subunit protein L16	136
rpmC	*b3312*	−4	50S ribosomal subunit protein L29	63
Cell processes				
gadE (*yhiE*)	*b3512*	−12.1	ORF, hypothetical protein; related to resistance at low pH	175
hdeA	*b3510*	−9.8	ORF, hypothetical protein; acid resistance protein, possible chaperone, subunit of HdeA dimer, inactive form of acid resistance protein	110
ORFs with unknown function				
hdeB	*b3509*	−9.2	ORF, hypothetical protein; 10K-L protein, related to acid resistance protein of *Shigella flexneri*	112
hdeD	*b3511*	−9.8	ORF, hypothetical protein; protein involved in acid resistance	190
ybaW	*b0443*	−5.3	ORF, hypothetical protein	132
yciE	*b1257*	−4	ORF, hypothetical protein	168
ymgB	*b1166*	−4.3	ORF, hypothetical protein	88
ymgC	*b1167*	−4.3	ORF, hypothetical protein	82
yodC	*b1957*	−4	ORF, hypothetical protein	60

[a] CoA, coenzyme A.

DISCUSSION

In this study, the following lines of evidence show that YdgG is a putative transport protein that either enhances AI-2 secretion or inhibits AI-2 uptake in *E*. coli. (i) Since external AI-2 addition increases biofilm formation (19), if YdgG promotes AI-2 export or inhibits AI-2 uptake, it is expected that deletion of *ydgG* should increase biofilms since more AI-2 is internalized, and this was indeed the case (570-fold, Fig. 1). (ii) Deletion of *ydgG* led to both a decrease in external AI-2 (13-fold) and an increase (10-fold) in internal AI-2 (Fig. 3); both results

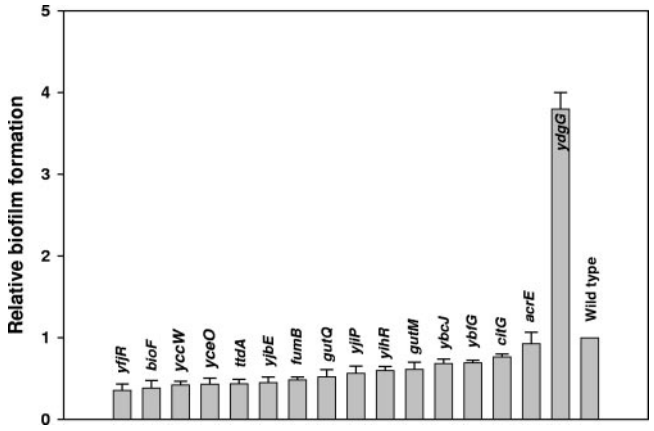

FIG. 5. Effects of selected deletions on *E. coli* biofilm formation in 96-well plates after 24 h in LB glu. The experiment was done in duplicate, and 1 standard deviation is shown.

indicate that YdgG influences the export of AI-2 or inhibits AI-2 uptake. A higher intracellular AI-2 concentration may lead to more AI-2 species being phosphorylated by LsrK, leading to *lsr* operon induction. (iii) The gene expression pattern in the biofilm observed here upon deletion of *ydgG* resembles the gene expression pattern observed for restoring *luxS* (net effect of AI-2 addition to suspended cultures) (49, 58); hence, YdgG influences a large number of genes, which is expected for the transporter of AI-2. (iv) The quorum-sensing regulator *qseB* is clearly observed to be induced upon deletion of *ydgG* under exponential growth conditions (Fig. 2), and *qseB* has been shown in our lab to be induced by enzymatically synthesized AI-2 (19); hence, if YdgG is inactive, either less AI-2 leaves the cell or more AI-2 is internalized, and one would expect AI-2-controlled genes like *qseB* to be up-regulated. (v) AI-2 controls motility and chemotaxis genes (49, 58); hence, if YdgG influences AI-2 secretion, upon deletion of ydgG, larger intracellular AI-2 concentrations should lead to higher motility, and sixfold more motility was found with the *ydgG* mutant here. (vi) The predicted secondary protein structure shows that YdgG is most likely to be a transport membrane protein. (vii) YdgG is highly conserved in other bacteria (72 genera have homologs), and 9 of the 11 genera that have the most-closely related YdgG homologs have LuxS homologs (e.g., *Shigella*, *Salmonella*, *Yersinia*, *Shewanella*, *Pasteurella*, *Haemophilus*, *Mannheimia*, *Actinobacillus*, and *Chromohalobacter*). (viii) Corroborating the prediction of YdgG as a transport protein, an increase in drug resistance was observed upon deletion of *ydgG*. (ix) The proximity of *ydgG* to both *ydgEF*, which encodes a multidrug resistance efflux protein (this locus is adjacent to *ydgG*) (40), and *ydgI*, which encodes an AcrD protein similar to an arginine-ornithine transporter in *Pseudomonas aeruginosa* (6) (four genes downstream from *ydgG*), supports the notion that YdgG is involved in transport. These results suggest that YdgG controls the efflux of AI-2 and fit well with the suggestion that AcrAB of *E. coli* effluxes quorum signals (45) and with the evidence that the MexAB-OprM multidrug efflux system of *P. aeruginosa* effluxes the quorum signal *N*-(3-oxododecanoyl)-L-homoserine lactone (17, 42).

The increase in biofilm formation by the *ydgG* mutant only when glucose was added to the medium may be attributed to greater differences in intracellular AI-2 production between the *ydgG* mutant and the wild-type strain (Fig. 3) than when glucose was absent. This result agrees with the increase in AI-2 synthesis upon addition of glucose to the growth medium due to catabolic repression by decreasing the levels of cAMP-cAMP receptor protein (65). Previous reports (60, 65) have shown that adding glucose increases extracellular AI-2 concentrations in mid- to late-exponential phase. Further study of differential gene expression of *ydgG* mutant biofilm cells in the absence of glucose may reveal the reason for the increase in biofilm formation only when glucose was added to the medium.

The greater biofilm formation of the *ydgG* mutant may also be due to induction of the indole secretion system *acrEF*, since similar genes have been related to biofilms previously; for example, Maira-Litrán et al. (36) showed that constitutive expression of *acrAB* protected *E. coli* biofilms from ciprofloxacin at 4 μg/liter. Additionally, it has been shown that genes related to the cell envelope and secretion are induced in biofilm cells compared to suspended cultures (5). The induction of *acrEF*, stationary-phase indole efflux-related genes, upon *ydgG* deletion and alteration of AI-2 secretion, fits well with our hypothesis that different signals control gene expression at different growth stages in *E. coli*: AI-2 for exponential-phase growth and an indole-related molecule for stationary-phase growth (50). Indeed, it appears that intracellular indole represses biofilms.

It should be pointed out that *ydgG* was found to be induced in *E. coli* JM109 biofilms containing the F′ conjugative plasmid (48) whereas the strains used in this study are F^-. Also, it has been reported that AI-2 is not necessary for biofilm formation in strains carrying conjugative plasmids (47). However, in this study, since AI-2 is necessary for biofilm formation (19), deletion of *ydgG* is shown to alter AI-2 transport and consequently to increase biofilm formation.

Gene expression in the biofilm of the *ydgG* mutant is consistent with the effect of adding AI-2 on the global gene expression in *E. coli* for suspension cells during exponential growth (49, 58) in that both conditions induce flagellum, motility, and chemotaxis genes. In addition, AI-2-repressible genes involved in growth and cell division (58) were also repressed in the *ydgG* mutant biofilms; for example, ribosomal genes such as *rplX*, *rplN*, *rplP*, *rplS*, *rplR*, *rpsK*, and *rpsT*. Also, growth-related genes such as *ftsA*, *ftsQ*, *fmt* (methionyl-tRNA formyltransferase), and *miaA* [tRNA delta(2)-isopentenylpyrophosphate] were repressed in both studies.

Typical related regulatory genes that were differentially expressed in the biofilm of the *ydgG* mutant are *rpoS* (repressed 2.8-fold, encodes the sigma factor σ^{38}) and *barA* (induced 3.24-fold, encodes a sensor kinase) (4). The RpoS regulon controls gene expression required for survival during starvation periods, transition between the exponential and stationary phases, heat shock, and cold shock (34); more than 100 genes are positively regulated by RpoS (41). We found 75% of the genes induced by RpoS in a stationary-phase suspended culture were repressed in the *ydgG* biofilm by more than 1.5-fold, and 72% of the genes repressed by RpoS were induced more than 1.5-fold in the *ydgG* biofilm.

In addition to the known biofilm-related genes induced in this study and the good agreement of the regulatory circuits involved in their expression, some uncharacterized genes re-

lated to biofilm formation in *E. coli* were identified in biofilms of the *ydgG* mutant. One highly induced operon in the *ydgG* mutant biofilm is the *gut* operon, which is related to the production of polysialic acid. *gutM* and *gutQ* were induced roughly 10-fold in the biofilm upon deletion of *ydgG*. *gutM* encodes the glucitol operon activator (70), and GutQ is similar to KpsF in *E. coli* K1, which plays a role in assembling the polysialic acid capsule virulence factor (9). Greiner et al. (20) found that 5-*N*-glycolylneuraminic acid (Neu5Ac), one of the building blocks of polysialic acid, is a constituent of *Haemophilus influenzae* biofilms. Also, Swords et al. (61) showed that sialylation promotes biofilm formation by *H. influenzae*. Further study may reveal that polysialic acid as an important component in *E. coli* and other species biofilms.

Genes related to anaerobic respiration were also highly induced upon deletion of *ydgG* and include those that are formate transport related (*focB* and *hyfACDR*). The significantly higher biomass in the *ydgG* mutant biofilm is likely to cause anaerobic conditions. Other genes related to anaerobic metabolism that are induced include *pflD*, encoding pyruvate formate-lyase (13.9-fold); *ttdA*, encoding L-tartrate dehydratase (13.9-fold); and *fumB* encoding fumarase B (9.2-fold). TtdA and FumB are enzymes for converting tartrate to oxaloacetate and malate to fumarate, respectively. There are three fumarase isozymes in *E. coli*, fumarases A, B, and C (products of *fumA*, *fumB*, and *fumC*, respectively). The cell adapts to changing environmental oxygen conditions by utilizing the different isozymes; hence, in the *ydgG* mutant biofilm, more biofilm may cause anaerobic conditions and *fumB* is relatively activated. TtdA is a stereospecific enzyme that is known to be induced during anaerobic growth with glycerol (46).

Among the induced genes (Table 2), more than 20 regulatory proteins were identified. The most induced was *yjiP* (103 aa, 20-fold). *alpA* was induced 6.5-fold and encodes a transcriptional activator related to phage functions (28). Differential gene expression of phage-related genes in biofilms has been reported for *Xylella fastidiosa* by de Souza et al. (15) on the basis of DNA microarrays. Also, Webb et al. (67) related phage functions and biofilms of *P. aeruginosa*. Further study needs to be done to establish the relationship of phage-related functions and biofilm formation in *E. coli*.

Also, 80% of the genes differentially expressed in a continuous reactor after 6 days of operation at a growth rate of 0.03/h (48) were also differentially expressed in the 24-h biofilm upon deletion of *ydgG*. This indicates the *ydgG* mutation causes the genes that are required for steady-state biofilm formation to be expressed, which results in greater biofilm formation.

We found 31% of the *E. coli* genome was differentially induced more than twofold in the *ydgG* mutant biofilm compared to the wild-type biofilm culture, and 8% of the genes were differentially repressed more than twofold. YdgG was found to repress cell surface determinants (genes related to flagellum, type 1 fimbria, Ag43, curli, and polysaccharide production), and it appears it controls these genes through AI-2 transport. Additionally, 10 genes previously not linked to biofilms were found here to influence biofilm formation in *E. coli*, and polysialic acid appears to have a role in the biofilm matrix. The results presented in this paper show that YdgG either enhances secretion of AI-2 or inhibits AI-2 uptake and that altering AI-2 intracellular concentrations affects global gene expression in the biofilms. Hence, we propose a new name for this locus: transport of quorum-sensing signal or *tqsA*. These results corroborate previous results that AI-2 is directly involved in biofilm formation (19) and imply that AI-2 must be actively transported from cells for cell signaling.

ACKNOWLEDGMENTS

We thank A. Heydorn of the Technical University of Denmark for kindly providing COMSTAT; S. Molin of the Technical University of Denmark for sending plasmid pCM18; Hirotada Mori of the Nara Institute of Science in Japan for sending the *E. coli* K-12 BW25113 mutants; James Kaper of the University of Maryland for sending plasmids pVS159, pVS176, pVS175, pVS182, and pVS183; and William E. Bentley of the University of Maryland for sending plasmid pLW11.

REFERENCES

1. **Baba, T., T. Ara, Y. Okumura, M. I. Hasegawa, Y. Takai, M. Baba, T. Oshima, M. Tomita, B. Wanner, and H. Mori.** Unpublished data.
2. **Balestrino, D., J. A. J. Haagensen, C. Rich, and C. Forestier.** 2005. Characterization of type 2 quorum sensing in *Klebsiella pneumoniae* and relationship with biofilm formation. J. Bacteriol. **187:**2870–2880.
3. **Bassler, B. L., M. Wright, R. E. Showalter, and M. R. Silverman.** 1993. Intercellular signalling in *Vibrio harveyi*: sequence and function of genes regulating expression of luminescence. Mol. Microbiol. **9:**773–786.
4. **Beloin, C., and J.-M. Ghigo.** 2005. Finding gene-expression patterns in bacterial biofilms. Trends Microbiol. **13:**16–19.
5. **Beloin, C., J. Valle, P. Latour-Lambert, P. Faure, M. Kzreminski, D. Balestrino, J. A. J. Haagensen, S. Molin, G. Prensier, B. Arbeille, and J.-M. Ghigo.** 2004. Global impact of mature biofilm lifestyle on *Escherichia coli* K-12 gene expression. Mol. Microbiol. **51:**659–674.
6. **Bourdineaud, J., D. Heierli, M. Gamper, H. Verhoogt, A. Driessen, W. Konings, C. Lazdunski, and D. Haas.** 1993. Characterization of the *arcD* arginine:ornithine exchanger of *Pseudomonas aeruginosa*. Localization in the cytoplasmic membrane and a topological model. J. Biol. Chem. **268:**5417–5424.
7. **Bru, C., E. Courcelle, S. Carrere, Y. Beausse, S. Dalmar, and D. Kahn.** 2005. The ProDom database of protein domain families: more emphasis on 3D. Nucleic Acids Res. **33:**D212–D215.
8. **Chilcott, G. S., and K. T. Hughes.** 2000. Coupling of flagellar gene expression to flagellar assembly in *Salmonella enterica* serovar Typhimurium and *Escherichia coli*. Microbiol. Mol. Biol. Rev. **64:**694–708.
9. **Cieslewicz, M., and E. Vimr.** 1997. Reduced polysialic acid capsule expression in *Escherichia coli* K1 mutants with chromosomal defects in *kpsF*. Mol. Microbiol. **26:**237–249.
10. **Cuff, J., M. Clamp, A. Siddiqui, M. Finlay, and G. Barton.** 1998. JPred: a consensus secondary structure prediction server. Bioinformatics **14:**892–893.
11. **Danese, P. N., L. A. Pratt, S. L. Dove, and R. Kolter.** 2000. The outer membrane protein, antigen 43, mediates cell-to-cell interactions within *Escherichia coli* biofilms. Mol. Microbiol. **37:**424–432.
12. **Danese, P. N., L. A. Pratt, and R. Kolter.** 2000. Exopolysaccharide production is required for development of *Escherichia coli* K-12 biofilm architecture. J. Bacteriol. **182:**3593–3596.
13. **Datsenko, K. A., and B. L. Wanner.** 2000. One-step inactivation of chromosomal genes in *Escherichia coli* K-12 using PCR products. Proc. Natl. Acad. Sci. USA **97:**6640–6645.
14. **Davies, D. G., M. R. Parsek, J. P. Pearson, B. H. Iglewski, J. W. Costerton, and E. P. Greenberg.** 1998. The involvement of cell-to-cell signals in the development of a bacterial biofilm. Science **280:**295–298.
15. **de Souza, A. A., M. A. Takita, H. D. Coletta-Filho, C. Caldana, G. M. Yanai, N. H. Muto, R. C. de Oliveira, L. R. Nunes, and M. A. Machado.** 2004. Gene expression profile of the plant pathogen *Xylella fastidiosa* during biofilm formation in vitro. FEMS Microbiol. Let. **237:**341–353.
16. **Di Martino, P., R. Fursy, L. Bret, B. Sundararaju, and R. S. Phillips.** 2003. Indole can act as an extracellular signal to regulate biofilm formation of *Escherichia coli* and other indole-producing bacteria. Can. J. Microbiol. **49:**443–449.
17. **Evans, K., L. Passador, R. Srikumar, E. Tsang, J. Nezezon, and K. Poole.** 1998. Influence of the MexAB-OprM multidrug efflux system on quorum sensing in *Pseudomonas aeruginosa*. J. Bacteriol. **180:**5443–5447.
18. **Freeman, J. A., and B. L. Bassler.** 1999. A genetic analysis of the function of LuxO, a two-component response regulator involved in quorum sensing in *Vibrio harveyi*. Mol. Microbiol. **31:**665–677.
19. **González Barrios, A. F., R. Zuo, Y. Hashimoto, L. Yang, W. E. Bentley, and T. K. Wood.** 2006. Autoinducer 2 controls biofilm formation in *Escherichia coli* K12 through a novel motility quorum-sensing regulator (MqsR, B3022). J. Bacteriol. **188:**305–316.
20. **Greiner, L. L., H. Watanabe, N. J. Phillips, J. Shao, A. Morgan, A. Zaleski, B. W. Gibson, and M. A. Apicella.** 2004. Nontypeable *Haemophilus influenzae*

strain 2019 produces a biofilm containing *N*-acetylneuraminic acid that may mimic sialylated O-linked glycans. Infect. Immun. **72:**4249–4260.
21. **Hammer, B. K., and B. L. Bassler.** 2003. Quorum sensing controls biofilm formation in *Vibrio cholerae*. Mol. Microbiol. **50:**101–104.
22. **Hansen, M. C., R. J. Palmer, Jr., C. Udsen, D. C. White, and S. Molin.** 2001. Assessment of GFP fluorescence in cells of *Streptococcus gordonii* under conditions of low pH and low oxygen concentration. Microbiology **147:**1383–1391.
23. **Henke, J. M., and B. L. Bassler.** 2004. Three parallel quorum-sensing systems regulate gene expression in *Vibrio harveyi*. J. Bacteriol. **186:**6902–6914.
24. **Heydorn, A., A. T. Nielsen, M. Hentzer, C. Sternberg, M. Givskov, B. K. Ersboll, and S. Molin.** 2000. Quantification of biofilm structures by the novel computer program COMSTAT. Microbiology **146:**2395–2407.
25. **Jones, D. T.** 1998. Do transmembrane protein superfolds exist? FEBS Lett. **423:**281–285.
26. **Jones, D. T., W. R. Taylor, and J. M. Thornton.** 1994. A model recognition approach to the prediction of all-helical membrane protein structure and topology. Biochemistry **33:**3038–3049.
27. **Kawamura-Sato, K., K. Shibayama, T. Horii, Y. Iimuma, Y. Arakawa, and M. Ohta.** 1999. Role of multiple efflux pumps in *Escherichia coli* in indole expulsion. FEMS Microbiol. Let. **179:**345–352.
28. **Kirby, J. E., J. E. Trempy, and S. Gottesman.** 1994. Excision of a P4-like cryptic prophage leads to Alp protease expression in *Escherichia coli*. J. Bacteriol. **176:**2068–2081.
29. **Klemm, P., L. Hjerrild, M. Gjermansen, and M. A. Schembri.** 2004. Structure-function analysis of the self-recognizing antigen 43 autotransporter protein from *Escherichia coli*. Mol. Microbiol. **51:**283–296.
30. **Kobayashi, K., N. Tsukagoshi, and R. Aono.** 2001. Suppression of hypersensitivity of *Escherichia coli acrB* mutant to organic solvents by integrational activation of the *acrEF* operon with the IS*1* or IS*2* element. J. Bacteriol. **183:**2646–2653.
31. **Krogh, A., B. Larsson, G. von Heijne, and E. L. L. Sonnhammer.** 2001. Predicting transmembrane protein topology with a hidden Markov model: application to complete genomes. J. Mol. Biol. **305:**567–580.
32. **Labbate, M., S. Y. Queck, K. S. Koh, S. A. Rice, M. Givskov, and S. Kjelleberg.** 2004. Quorum-sensing-controlled biofilm development in *Serratia liquefaciens* MG1. J. Bacteriol. **186:**692–698.
33. **Lazazzera, B. A.** 2005. Lessons from DNA microarray analysis: the gene expression profile of biofilms. Curr. Opin. Microbiol. **8:**222–227.
34. **Loewen, P. C., B. Hu, J. Strutinsky, and R. Sparling.** 1998. Regulation in the *rpoS* regulon of *Escherichia coli*. Can. J. Microbiol. **44:**707–717.
35. **Ma, D., D. Cook, M. Alberti, N. Pon, H. Nikaido, and J. Hearst.** 1993. Molecular cloning and characterization of *acrA* and *acrE* genes of *Escherichia coli*. J. Bacteriol. **175:**6299–6313.
36. **Maira-Litrán, T., D. G. Allison, and P. Gilbert.** 2000. An evaluation of the potential of the multiple antibiotic resistance operon (*mar*) and the multidrug efflux pump *acrAB* to moderate resistance towards ciprofloxacin in *Escherichia coli* biofilms. J. Antimicrob. Chemother. **45:**789–795.
37. **McGinnis, S., and T. L. Madden.** 2004. BLAST: at the core of a powerful and diverse set of sequence analysis tools. Nucleic Acids Res. **32:**W20–W25.
38. **McGuffin, L. J., K. Bryson, and D. T. Jones.** 2000. The PSIPRED protein structure prediction server. Bioinformatics **16:**404–405.
39. **McNab, R., S. K. Ford, A. El-Sabaeny, B. Barbieri, G. S. Cook, and R. Lamont.** 2003. LuxS-based signaling in *Streptococcus gordonii*: autoinducer 2 controls carbohydrate metabolism and biofilm formation with *Porphyromonas gingivalis*. J. Bacteriol. **185:**274–284.
40. **Nishino, K., and A. Yamaguchi.** 2001. Analysis of a complete library of putative drug transporter genes in *Escherichia coli*. J. Bacteriol. **183:**5803–5812.
41. **Patten, C. L., M. G. Kirchhof, M. R. Schertzberg, R. A. Morton, and H. E. Schellhorn.** 2004. Microarray analysis of RpoS-mediated gene expression in *Escherichia coli* K-12. Mol. Gen. Genomics **272:**580–591.
42. **Pearson, J. P., C. Van Delden, and B. H. Iglewski.** 1999. Active efflux and diffusion are involved in transport of *Pseudomonas aeruginosa* cell-to-cell signals. J. Bacteriol. **181:**1203–1210.
43. **Pratt, L. A., and R. Kolter.** 1998. Genetic analysis of *Escherichia coli* biofilm formation: roles of flagella, motility, chemotaxis and type I pili. Mol. Microbiol. **30:**285–293.
44. **Prigent-Combaret, C., G. Prensier, T. T. Le Thi, O. Vidal, P. Lejeune, and C. Dorel.** 2000. Developmental pathway for biofilm formation in curli-producing *Escherichia coli* strains: role of flagella, curli and colanic acid. Environ. Microbiol. **2:**450–464.
45. **Rahmati, S., S. Yang, A. L. Davidson, and E. L. Zechiedrich.** 2002. Control of the AcrAB multidrug efflux pump by quorum-sensing regulator SdiA. Mol. Microbiol. **43:**677–685.
46. **Reaney, S. K., C. Begg, S. J. Bungard, and J. R. Guest.** 1993. Identification of the L-tartrate dehydratase genes (*ttdA* and *ttdB*) of *Escherichia coli* and evolutionary relationship with the class I fumarase genes. J. Gen. Microbiol. **139:**1523–1530.
47. **Reisner, A., J. A. J. Haagensen, M. A. Schembri, E. L. Zechner, and S. Molin.** 2003. Development and maturation of *Escherichia coli* K-12 biofilms. Mol. Microbiol. **48:**933–946.
48. **Ren, D., L. A. Bedzyk, S. M. Thomas, R. W. Ye, and T. K. Wood.** 2004. Gene expression in *Escherichia coli* biofilms. Appl. Microbiol. Biotechnol. **64:**515–524.
49. **Ren, D., L. A. Bedzyk, R. W. Ye, S. M. Thomas, and T. K. Wood.** 2004. Differential gene expression shows natural brominated furanones interfere with the autoinducer-2 bacterial signaling system of *Escherichia coli*. Biotechnol. Bioeng. **88:**630–642.
50. **Ren, D., L. A. Bedzyk, R. W. Ye, S. M. Thomas, and T. K. Wood.** 2004. Stationary-phase quorum-sensing signals affect autoinducer-2 and gene expression in *Escherichia coli*. Appl. Environ. Microbiol. **70:**2038–2043.
51. **Ren, D., J. J. Sims, and T. K. Wood.** 2001. Inhibition of biofilm formation and swarming of *Escherichia coli* by (*5Z*)-4-bromo-5-(bromomethylene)-3-butyl-2(*5H*)-furanone. Environ. Microbiol. **3:**731–736.
52. **Ren, D., R. Zuo, A. F. Gonzalez Barrios, L. A. Bedzyk, G. R. Eldridge, M. E. Pasmore, and T. K. Wood.** 2005. Differential gene expression for investigation of *Escherichia coli* biofilm inhibition by plant extract ursolic acid. Appl. Environ. Microbiol. **71:**4022–4034.
53. **Rodriguez, R. L., and R. C. Tait.** 1983. Recombinant DNA techniques: an introduction. Benjamin/Cummings Publishing, Menlo Park, Calif.
54. **Rost, B., G. Yachdav, and J. Liu.** 2004. The PredictProtein server. Nucleic Acids Res. **32:**W321–W326.
55. **Sambrook, J., E. F. Fritsch, and T. Maniatis.** 1989. Molecular cloning: a laboratory manual, 2nd ed. Cold Spring Harbor Laboratory Press, Cold Spring Harbor, N.Y.
56. **Schembri, M. A., K. Kjærgaard, and P. Klemm.** 2003. Global gene expression in *Escherichia coli* biofilms. Mol. Microbiol. **48:**253–267.
57. **Sonnhammer, E. L., G. von Heijne, and A. Krogh.** 1998. A hidden Markov model for predicting transmembrane helices in protein sequences. Proc. Int. Conf. Intell. Syst. Mol. Biol. **6:**175–182.
58. **Sperandio, V., A. G. Torres, J. A. Giron, and J. B. Kaper.** 2001. Quorum sensing is a global regulatory mechanism in enterohemorrhagic *Escherichia coli* O157:H7. J. Bacteriol. **183:**5187–5197.
59. **Sperandio, V., A. G. Torres, and J. B. Kaper.** 2002. Quorum sensing *Escherichia coli* regulators B and C (QseBC): a novel two-component regulatory system involved in the regulation of flagella and motility by quorum sensing in *Escherichia coli*. Mol. Microbiol. **43:**809–821.
60. **Surette, M. G., and B. L. Bassler.** 1998. Quorum sensing in *Escherichia coli* and *Salmonella typhimurium*. Proc. Natl. Acad. Sci. USA **95:**7046–7050.
61. **Swords, W. E., M. L. Moore, L. Godzicki, G. Bukofzer, M. J. Mitten, and J. VonCannon.** 2004. Sialylation of lipooligosaccharides promotes biofilm formation by nontypeable *Haemophilus influenzae*. Infect. Immun. **72:**106–113.
62. **Taga, M. E., S. T. Miller, and B. L. Bassler.** 2003. Lsr-mediated transport and processing of AI-2 in *Salmonella typhimurium*. Mol. Microbiol. **50:**1411–1427.
63. **Taga, M. E., J. L. Semmelhack, and B. L. Bassler.** 2001. The LuxS-dependent autoinducer AI-2 controls the expression of an ABC transporter that functions in AI-2 uptake in *Salmonella typhimurium*. Mol. Microbiol. **42:**777–793.
64. **Wang, D., X. Ding, and P. N. Rather.** 2001. Indole can act as an extracellular signal in *Escherichia coli*. J. Bacteriol. **183:**4210–4216.
65. **Wang, L., Y. Hashimoto, C.-Y. Tsao, J. J. Valdes, and W. E. Bentley.** 2005. Cyclic AMP (cAMP) and cAMP receptor protein influence both synthesis and uptake of extracellular autoinducer 2 in *Escherichia coli*. J. Bacteriol. **187:**2066–2076.
66. **Wang, X., J. F. Preston III, and T. Romeo.** 2004. The *pgaABCD* locus of *Escherichia coli* promotes the synthesis of a polysaccharide adhesin required for biofilm formation. J. Bacteriol. **186:**2724–2734.
67. **Webb, J. S., L. S. Thompson, S. James, T. Charlton, T. Tolker-Nielsen, B. Koch, M. Givskov, and S. Kjelleberg.** 2003. Cell death in *Pseudomonas aeruginosa* biofilm development. J. Bacteriol. **185:**4585–4592.
68. **Wood, T. K., and S. W. Peretti.** 1991. Effect of chemically induced, cloned-gene expression on protein synthesis in *E. coli*. Biotechnol. Bioeng. **38:**397–412.
69. **Xavier, K. B., and B. L. Bassler.** 2005. Regulation of uptake and processing of the quorum-sensing autoinducer AI-2 in *Escherichia coli*. J. Bacteriol. **187:**238–248.
70. **Yamada, M., and M. H. J. Saier.** 1988. Positive and negative regulators for glucitol (*gut*) operon expression in *Escherichia coli*. J. Mol. Biol. **203:**569–583.
71. **Yeh, K. S., J. K. Tinker, and S. Clegg.** 2002. FimZ binds the *Salmonella typhimurium fimA* promoter region and may regulate its own expression with FimY. Microbiol. Immunol. **46:**1–10.
72. **Zhu, J., and J. J. Mekalanos.** 2003. Quorum sensing-dependent biofilms enhance colonization in *Vibrio cholerae*. Dev. Cell **5:**647–656.